課題名：高速 QXAFS 測定による金属ナノ粒子の生成過程の in situ 観察
In situ observation of metal nanoparticle formation process by high-speed QXAFS measurement

京都大学大学院工学研究科　博士後期課程 3 回生　大山順也

Abstract

The formation of gold nanoparticles in the presence of dodecanethiol was observed *in situ* by quick X-ray absorption fine structure spectroscopy with 100 ms time resolution at the Au L_3 and L_2 edges. The series of the X-ray absorption near edge structure spectra at both edges was analysed to evaluate the dispersion and electronic properties of gold nanoparticles during their growth.

Introduction

Interest in the study of gold nanoparticles (AuNPs) is increasing because of their unique properties not observed in bulk material.[1-3] In particular, AuNPs with diameters of less than 2 nm show a property different not only from the bulk but also larger NPs.[2, 4] Therefore, great efforts using various protective agents and under various conditions have been made to control the size and structure of AuNPs.[4-8] Thiol is known as one of the most useful protective agents to control the size and structure of AuNPs, since the report by Brust *et al.*,[5] and size-controlled synthesis can be easily attained by varying the initial molar ratio of thiol to Au ions.[6, 9, 10] Recently, atomically precise thiolate protecting gold nanoparticles with diameters of less than 2 nm, $Au_m(SR)_n$, with new properties, such as catalytic activity, chemical stability, magnetic properties, and optical properties, have been synthesized.[1] To elucidate these unique properties, it is important to investigate their structures and electronic states.

  X-ray absorption spectroscopy (XAS) is often utilized in metal NP characterization.[11, 12] Zanchet *et al.* clarified that the strong Au–S interaction compensates for the expected lattice contraction in free AuNPs.[13] Sham *et al.* reported that AuNPs lose *d* electrons when protected by thiolate, which strongly interacts with gold, although they gain electrons in their 5*d* orbitals when protected by weakly interacting dendrimers.[14]. They also revealed that *d* electrons of the thiolate-protected AuNPs decrease with a decrease in their size.[15] MacDonald *et al.* precisely determined the structure of $Au_{144}(SR)_{60}$ and investigated the size-dependant nature of bonding by comparing it with $Au_m(SR)_n$.[16] In these studies on the electronic properties of thiol-protected AuNPs, the Mansour's method was employed. However, this method assumes that there is no significant orbital hybridization. Thus, we should more closely investigate X-ray absorption near edge structure (XANES) spectra of thiol-protected AuNPs using Mansour's method.

  Recently, we reported the *in situ* observation of formation of AuNPs using dodecanethiol (DT) as a protecting agent in solution by quick X-ray absorption fine structure (QXAFS) spectroscopy with a 100 ms time resolution.[17] It is proposed that all Au ions in solution are reduced by $NaBH_4$ at a

burst to form very small Au clusters, the nuclei, followed by their aggregation to form AuNPs.[17, 18] In other words, we can observe AuNPs of various sizes, from sub-nanometre to several nanometres, during their growth. As a result, in this study, the variation of electronic properties with AuNP size is investigated by *in situ* observations of particle formation.

Experimental section

Preparation and XAFS measurement

We added 2 mL of aqueous $HAuCl_4$ (0.129 M) and 2.58 mL of toluene to a round bottom flask, followed by the addition of tetraoctylammonium bromide (TOAB) (282 mg, 0.516 mmol). This resulted in the transfer of $AuCl_4^-$ from aqueous $HAuCl_4$ to toluene to form $[TOA]AuCl_4$. Next 0.2 mL of toluene solution containing $AuCl_4^-$ (0.1 M), 0.2 mL of toluene solution containing DT (0.1 M) and 1.2 mL of toluene were added to a Teflon cell (optical path length: 8 mm), in which concentrations of $AuCl_4^-$ and DT were 0.0125 M (DT/Au = 1). The solution in the Teflon cell was cooled to 263 K using a USP-203-A variable temperature liquid nitrogen cryostat (UNISOKU Co., Ltd.). To this solution, 0.4 mL of *N,N'*-dimethylformamide (DMF) solution of $NaBH_4$ (0.1 M) was added using an electromagnetic valve.

The QXAFS experiment of the Au L_3 and L_2 edges was performed on the BL40XU beamline in SPring-8 of the Japan Synchrotron Radiation Research Institute (JASRI; 8 GeV, 100 mA), wherein high-flux X-rays are supplied using a helical undulator.[19] The spectra were measured in the transmission mode. A small and light Si (111) monochromator was used to achieve millisecond time resolution. The XAFS measurements were performed with a 100 ms time resolution. After 10 spectra were collected, the *in situ* XAFS measurement was triggered at the same time as the addition of DMF solution of $NaBH_4$ to the toluene solution. The spectra were measured for 180 s to obtain 1800 spectra. XAFS spectra of good quality were selected and accumulated for each 1 s time interval to obtain a series of spectra. Spectra of Au foil (0.1 μm) were measured simultaneously for energy calibration. The Au L_3- and L_2-edge XANES spectral measurements were performed separately. Data reduction was performed using the REX2000 Ver.2.5.9. program (Rigaku). As a reference, $Au_{11}(PPh_3)_8Cl_3$ was prepared as described previously.[20] $Au_{11}(PPh_3)_8Cl_3$ was identified using UV-vis and XAFS spectroscopies.[21] The solution of DT/Au = 2, in which a Au atom existed as $[TOA]Au^+Cl$,[22] was also prepared as a reference.

Characterization of electronic properties

The XANES spectra were analysed according to Mansour's method to calculate the parameters for the number of *d* band vacancies, although the parameters may not have a clear correlation with the number of *d* band vacancies in the present case, i.e. DT-protected AuNPs.[11] The L_3 and L_2 XAFS spectra of the Au foil were normalized such that the both extended XAFS (EXAFS) oscillations symmetrically overlap one another at more than 40 eV above the X-ray absorption edge. The areas were determined using the part of the XANES spectrum that extended from 10 eV below the edge to

15 eV above the edge using Simpson's method. The L_3 and L_2 edge areas for the Au foil, A_{3r} and A_{2r}, were 1.064×10^4 and 1.67×10^3 eVcm^{-1}, respectively, and were determined using the absorption cross sections for the edges, 107.7 and 57.3 cm^{2}g^{-1} for the L_3 and L_2 edges, respectively.

The fractional change in the number of d band vacancies (unoccupied d states) from those of the bulk Au, f_d, was defined as

$$f_d = \Delta h_T/(h_T)_{\text{bulk Au}} = (\Delta A_3 + 1.11\Delta A_2)/(A_3 + 1.11A_2)_{\text{bulk Au,}} \qquad (1)$$

where $\Delta h_T = (h_T)_{\text{sample}} - (h_T)_{\text{bulk Au}}$; $\Delta A_j = (A_j)_{\text{sample}} - (A_j)_{\text{bulk Au}}$; h_T is the total number of unoccupied d states; and A_j is the edge area for the jth edge.

The h_T value was calculated using the following equation [a rearrangement of Eq. (1)]:

$$h_T = (1 + f_d) \, h_{Tr}. \qquad (2)$$

Changes in the vacancies in the $d_{5/2}$ and $d_{3/2}$ states were calculated using the following expressions:

$$\Delta h_{5/2} = (2.25\Delta A_3 - 0.5\Delta A_2)/C, \qquad (3)$$

$$\Delta h_{3/2} = 3 \, \Delta A_2/C, \qquad (4)$$

where C is the constant characteristic of the absorption (C = 75213 eVcm^{-1}).[23]

Results and Discussion

Dispersion

Figure 1(a) shows the series of Au L_3-edge XANES spectra during particle formation together with those of the [TOA]AuCl$_4$ in toluene (Au^{3+} solution) and the Au foil. The XANES spectrum of the Au^{3+} solution had a sharp and narrow absorption band around the edge (1192 eV), which is called the white line. The band corresponded to the electronic transition from the $2p_{3/2}$ core level state to the vacant $5d_{3/2}$ and $5d_{5/2}$ states. The XANES spectrum of the Au foil exhibited almost no white line because of the almost completely filled $5d$ state of Au^0. The solution of DT/Au = 1 before the addition of NaBH$_4$ had a smaller white line than that of the Au^{3+} solution because of the reduction of an Au^{3+} ion by two molecules of DT to an Au$^+$ ion.[22] In other words, the solution of DT/Au = 1 before the addition of NaBH$_4$ contained an equal quantity of Au$^+$ and Au^{3+} ions, which was confirmed by least-squares fitting of the XANES spectrum before reduction with a linear combination of Au^{3+} and Au$^+$ solutions.[17] The white line of the solution of DT/Au = 1 disappeared immediately after the addition of NaBH$_4$, and alternatively, a small and broad peak appeared just at the high-energy side of the edge (11929 eV). The peak intensity became the strongest at 3.6 s. Previously, the XANES spectrum with a small and broad peak was assigned to very small Au clusters during particle formation, i.e. nuclei.[17] The intensity of the peak at 3.6 s decreased with time, and the two broad bands at 11948 and 11970 eV appeared. In short, the XANES spectra became similar to that of the Au foil. The spectral change indicated the reduction of Au ions and formation of AuNPs. Figure 1(b) shows the series of the Au L_2-edge XANES spectra together with those of the Au^{3+} solution and Au foil. The L_2-edge XANES spectra of the Au^{3+} solution also showed the white line at 13735 eV, which was assigned to the electronic transition from $2p_{1/2}$ to $5d_{3/2}$. The white line intensity was smaller than that at the L_3-edge because the white line at the L_2-edge was

indicative of unoccupied $d_{3/2}$ state, and that at the L_3-edge was indicative of unoccupied $d_{3/2}$ and $d_{5/2}$ states. Analysis of the L_2-edge XANES spectrum indicated that the Au atoms in the solution of DT/Au = 1 before reduction consisted of an equal quantity of Au$^+$ and Au^{3+} ions, which was the same result as that indicated by L_3 spectral analysis. The spectral change at the L_2 edge showed the same behaviour as that at the L_3 edge: immediate disappearance of the white line on the addition of NaBH$_4$; appearance of a small and broad peak at the high-energy side of the edge (13742 eV); decrease in the intensity of the peak from 3.6 s and appearance of the two small peaks at 13760 and 13783 eV, approaching those of the spectrum of the Au foil. Thus, we successfully observed the spectral changes during AuNPs formation not only at the Au L_3 edge but also at the Au L_2 edge. Here the influence of DT on particle growth should be mentioned. The spectra of the Au nuclei observed at 3.6 s had a small and broad peak around the edges, which was characteristic of the AuNPs with Au–S bonds. Thus, DT trapped the gold clusters from the beginning of the growth, which led to slower particle growth in comparison to the growth without DT.
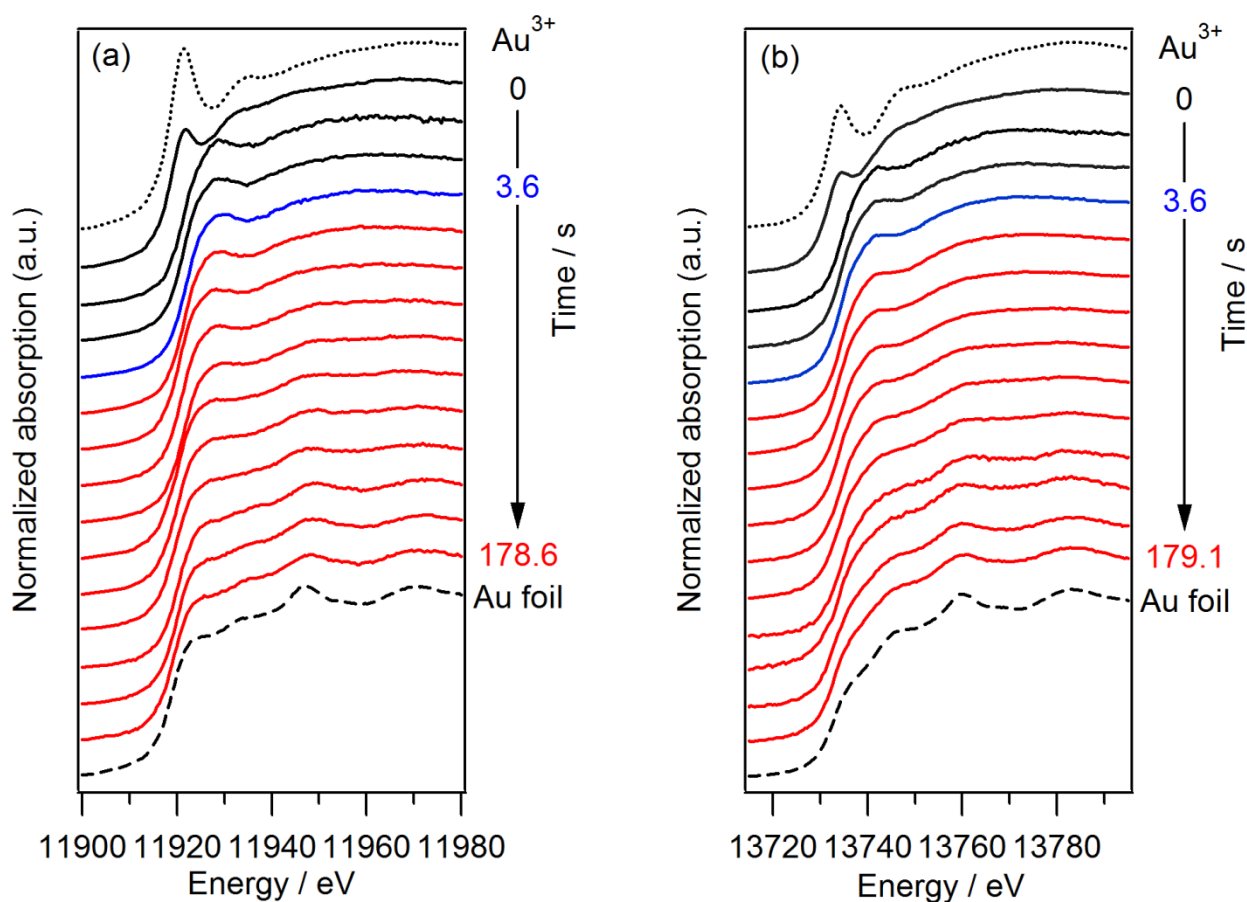

Figure 1. The series of XANES spectra at the (a) Au L_3 and (b) L_2 edges during particle formation (solid lines) together with those of HAuCl$_4$ in DMF (Au^{3+} solution) (dotted line) and Au foil (dashed line). The series of spectra during particle formation and that of the Au^{3+} solution are shifted vertically for clarity.

The series of the Au L_3-edge XANES spectra from 3.6 s to 178.6 s were fitted with the linear combination of the spectrum of the Au nuclei (observed at 3.6 s) and that of the Au foil were fitted using the least-squares method as well as the Au L_2-edge XANES spectra from 3.6 s to 179.1 s, which was verified by factor analysis. Figure 2 shows the time course of the fractions of the spectrum at 3.6 s and that of the Au foil resulting from the fit. The fractions of L_3-edge XANES spectra were almost the same as those of L_2-edge XANES spectra. The fractions of the Au nuclei and foil spectra decreased and increased, respectively, with time and approached approximately 70% and 30%. We interpreted the fractions of the Au nuclei and Au foil spectra as those of the surface and inner atoms of the AuNPs, respectively, as reported previously.[17] On the basis of this interpretation, the fractions of the surface and inner atoms decreased and increased with reaction time, respectively, indicating the growth of AuNPs from Au nuclei. The fraction of Au foil at 180 s was less than 100%, indicating the formation of AuNPs because AuNPs had a higher surface fraction than the Au foil. We should also note that almost all the Au atoms in the reaction solution comprised the Au nuclei at 3.6 s because the Au nuclei were observed by XAFS spectroscopy, which provides information on the average state of the absorption atom. These results suggested that AuNPs grow via the aggregation of AuNPs themselves.[17, 18] As a result, we can estimate the particle size from the fraction of surface atoms, or, in other words, the dispersion.
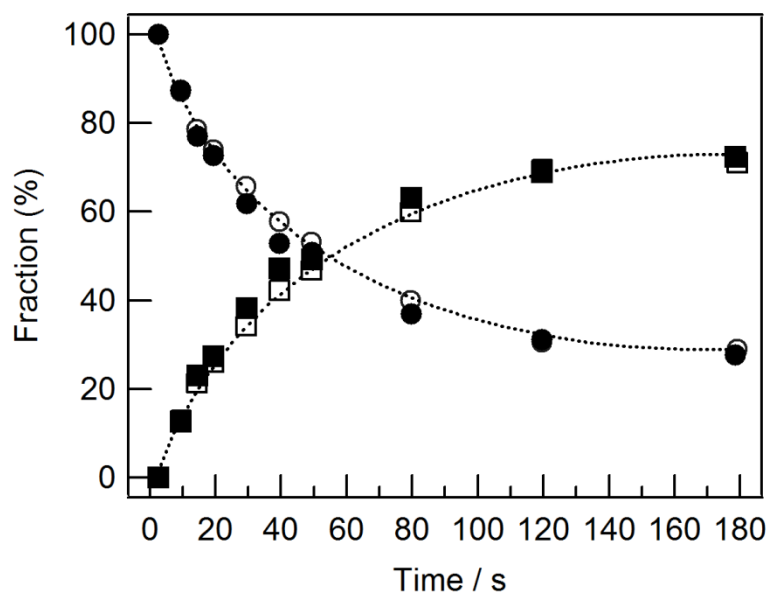

Figure 2. Time course of the fraction of the XANES spectrum of the Au nuclei observed at 3.6 s (representing the surface atoms) (circle) and that of the Au foil (representing the inner atoms) (square) after 3.6 s. The fractions were evaluated by least-squares fitting of the series of XANES spectra at the Au L_3 (unfilled) and L_2 edges (filled) with a linear combination of those of the Au nuclei and Au foil. The resulting R factors are 0.4%‑1%.

Electronic state

The series of Au L_3 and L_2 XANES spectra during particle growth from 3.6 to 180 s showed a higher absorption intensity than the Au foil in the energy region from the edge to 15 eV above the edge. Such a spectral feature is characteristic of XANES spectra of DT-protected AuNPs, as described previously.[14-16] The higher absorption intensities for AuNPs at the edges are probably because of the larger d band vacancies of the Au atoms of AuNPs than the Au foil. The d band vacancies result from electron transfer from the Au atoms to the adsorbed S atoms of DT.[24] According to this assumption, we analysed the series of the Au L_3- and L_2-edge XANES spectra after formation of the Au nuclei at 3.6 s to evaluate the h parameters for the number of d band vacancies. The h parameters were evaluated from the different absorption areas between the XANES spectra of a sample and the Au foil at the L_3 and L_2 edges in the energy region from 10 eV below the edge to 15 eV above the edge (ΔA_3 and ΔA_2) using established equations (Eqs. 1–4), assuming that the number of unoccupied d states per Au atom for bulk Au in total (h_T), in the $d_{5/2}$ state ($h_{5/2}$) and in the $d_{3/2}$ state ($h_{3/2}$) was 0.401, 0.283 and 0.118, respectively.[25] Table 1 summarizes the representative results. The spectrum of $Au_{11}(PPh_3)_8Cl_3$ was also analysed as a reference. The h_T of the Au nuclei (0.525) was slightly larger than that of the $Au_{11}(PPh_3)_8Cl_3$, indicating the generation of small Au clusters such as the Au_{11} cluster at 3.6 s. This was in accordance with our previous proposal of the generation of an Au_4 cluster as an Au nucleus.[17] The h_T decreased with reaction time, in other words, with the size of the AuNPs. The dependence of the h_T value on size was compatible with the results of Zhang *et al.*, who showed that the percentage of d band vacancies decreased with the size of DT-protected AuNPs (1.6 nm > 2.4 nm > 4.0 nm),[15], and also with the results of MacDonald *et al.*, who investigated changes in the number of d band vacancies of $Au_{25}(SR)_{18}$, $Au_{38}(SR)_{24}$ and $Au_{144}(SR)_{60}$ relative to bulk Au to clarify the fact that the smaller clusters have larger vacancies in the d band.[16] We concluded that the analysis described above is an appropriate method for evaluation of size-dependant XANES spectra of thiolate-protected AuNPs.

Interestingly, the difference in $h_{3/2}$ between the sample and Au foil, $\Delta h_{3/2}$, showed a larger value than $\Delta h_{5/2}$ at every time as listed in Table 1. In general, $\Delta h_{3/2}$ should have had a smaller value than $\Delta h_{5/2}$ for the following reasons: (1) splitting of the d states due to spin-orbit coupling results in $d_{5/2}$ states at higher energies and $d_{3/2}$ states at lower energies and (2) d vacancies are distributed from higher to lower energies. In the case of Au metal, there are slight d vacancies, which should be largely distributed in the $d_{5/2}$ states. However, $\Delta h_{5/2}$ was not larger than $\Delta h_{3/2}$ in this case. Zhang *et al.* also pointed out that $\Delta h_{3/2}$ for DT-protected AuNPs had a slightly larger value than $\Delta h_{5/2}$.[14] On the basis of the general understanding of the density of states in the d band, we concluded that h_T, $h_{5/2}$ and $h_{3/2}$ evaluated from XANES spectral analysis of AuNPs reflected only the number of d band vacancies. The other factors concerned the small and broad bands around the edges in the XANES spectra of the DT-protected AuNPs.

Table 1. The parameters of AuNPs evaluated from the XANES spectra.

Sample [a]	ΔA_3 eVcm^{-1}	ΔA_2 eVcm^{-1}	h_T	$h_{5/2}$	$h_{3/2}$	$\Delta h_{5/2}$	$\Delta h_{3/2}$	Dispersion (%) [b]
3.6 s	2138	1545	0.525	0.337	0.180	0.054	0.062	100
9.5 s	1750	1374	0.506	0.326	0.173	0.043	0.055	87.2
19.5 s	1693	1093	0.494	0.326	0.162	0.043	0.044	73.3
39.5 s	1067	711	0.461	0.310	0.146	0.027	0.028	55.3
79.6 s	631	698	0.446	0.297	0.146	0.014	0.028	38.4
178.9 s	309	492	0.428	0.289	0.138	0.006	0.020	28.3
Au foil [c]	–	–	0.401	0.283	0.118	–	–	0
$Au_{11}(PPh_3)_8Cl_3$	2017	1141	0.506	0.336	0.164	0.053	0.046	91.0

(a) The average time for the L_3- and L_2-edge XANES spectra.

(b) The average dispersion evaluated from the L_3- and L_2-edge XANES spectra.

(c) Values from Ref. (25).

  On the other hand, scientists reported that chemisorptions of hydrogen induced changes in Au L_3- and L_2-edge XANES spectra of AuNP-supported metal oxides as well as in Pt L_3- and L_2-edge spectra of Pt nanopartices (PtNPs).[26-29] From the chemisorption of hydrogen, Au L_3- and L_2-edge XANES spectra showed higher X-ray absorption intensities in the energy region from the edge to ca. 15 eV above the edge, while the Pt L_3- and L_2-edge XANES spectra represented higher absorption intensities with the chemisorptions. The difference absorption spectrum at the L_3 edge between the spectra with and without chemisorptions displayed almost the same band as that at the L_2 edge. If d band vacancies are calculated from almost the same difference absorption spectra at L_3 and L_2 using the described procedure, $\Delta h_{3/2}$ should show a larger value than $\Delta h_{5/2}$, which is generally unacceptable because of the density of the d band state described above. Actually, the origin of the increase in the absorption intensity was probably due to the electronic transition to the anti-bonding orbital of the metal–H bonds or multiple scattering of adsorbed H atoms with partially negative charges.[27, 30, 31] However, in the case of DT-protected AuNPs, these bands are probably due to d band vacancies, and it is likely that the higher X-ray absorption intensity of AuNPs around the edges is mainly due to electronic transition to unoccupied orbitals of the Au–S bonds, in other words, Au-S scatterings.[26-28] In fact, the density functional calculation for the Au cluster reported by Nobusada presented the main atomic orbital consisting of Au(6s) and S(3s) as the LUMO.[32] Furthermore, the fact that [TOA]Au$^+$Cl, which does not have Au–S bonds, has no peak around the L_3 and L_2 edges also supported our proposal. Therefore, the values of h_T, $h_{5/2}$ and $h_{3/2}$ mainly reflected the scattering intensity of the Au–S pair and may contain information about d band vacancies.

  Considering the understanding of the values of $h_{5/2}$ and $h_{3/2}$, the values were plotted against dispersion as shown in Figure 3. The $h_{3/2}$ value almost linearly decreased with dispersion, indicating that the net vacancies in the $d_{3/2}$ states were too small to appear in the variation of $h_{3/2}$ in comparison

with the amplitude of Au–S scatterings. On the other hand, the value of $h_{5/2}$ also decreased with dispersion, however, not in a linear fashion. This result suggested that the value of $h_{5/2}$ reflected not only Au–S scatterings but also the electronic properties of AuNPs. Figure 4 shows the Au L_3- and L_2-edge XANES spectra at ca. 180 s with those synthesized by the linear combination of the Au nuclei at 3.6 s and the Au foil. The synthesized XANES spectrum at the L_3 edge showed a slightly stronger intensity than the experimental one in the energy region from the edge to 15 eV above the edge. The stronger intensity of the synthesized spectrum agreed with the non-linear decrease in the value of $h_{5/2}$ with dispersion, particularly at low dispersions. On the other hand, the synthesized spectrum at the L_2 edge also agreed with the measured one in the energy region from the edge to 15 eV above the edge, conforming to the linear decrease of $h_{3/2}$ with dispersion. We concluded that the value of $h_{5/2}$ reflected d band vacancies of AuNPs, and that of $h_{3/2}$ hardly signified it because of the large contribution of Au–S scatterings.
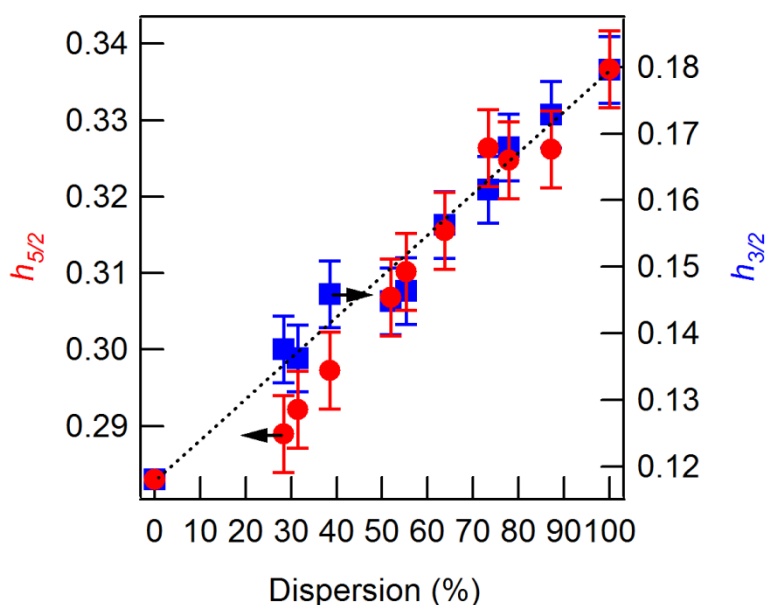

Figure 3. (a) The values of $h_{5/2}$ (circle) and (b) $h_{3/2}$ (square) plotted against dispersion evaluated from XANES spectral analysis.

Figure 5 displays the variation in the value of $h_{5/2}$ with the diameter of AuNPs. The diameter was estimated from dispersion evaluated by XANES analysis on the assumption of spherical AuNPs and a 0.288-nm Au atomic distance. In Figure 5, AuNPs with diameters more than 20 nm probably had the same value of d vacancies as that of bulk Au (The calculated dispersion of AuNPs with diameters of 20 nm was 8.4%). The value of $h_{5/2}$ did not increase according to the inverse of the diameter but exponentially increased with a decrease in the diameter. This change in the value of $h_{5/2}$ suggested that the electrons of the Au atoms were additionally transferred to the S atoms of DT as the size of AuNPs decreased. The additional electron transfer may be the intrinsic size effect of AuNPs. The

size-dependant catalytic activity has attracted much attention in catalysis science. Several reports state that catalytic activities deviated the size of AuNPs, for example, the oxidation of p-hydroxybenzaldehyde using poly(N-vinyl-2-pyrroridone) (PVP)-protected AuNPs and glucose oxidation of AuNPs supported by active carbon.[4, 33] These catalytic activities that deviated from the size are consistent with variations in the $h_{5/2}$ parameters of the size investigated in this study. The deviated electron transfer from the AuNPs to the adsorbate (DT) observed in this study probably contributed to the activation of O_2 in the catalytic reaction. In fact, it has been proposed that O_2 gains electrons to form the reactive oxygen species on AuNPs.[4, 34] On the other hand, in catalytic reactions on AuNPs supported by metal oxides, scientists have proposed that the contact structure of AuNPs with the metal oxide supports and the function of the supports largely contribute to reactivity.[35, 36] Metal oxide supports would have a more significant effect on the function of AuNPs than PVP and active carbon. However, it was also reported that AuNPs with diameters of 2 nm on TiO_2 show properties similar to those of Pt and Pd.[37] In addition, the unique catalytic activity of AuNPs was accounted for by the quantum size effect.[38, 39] These results suggested that the electronic property of AuNPs also contributes to the catalysis of AuNPs supported by metal oxides. Thus, evaluation of electronic properties of AuNPs is important in understanding the origin of unique properties. To understand this connection, we will conduct further studies for evaluating the electronic properties of AuNPs using XAS.
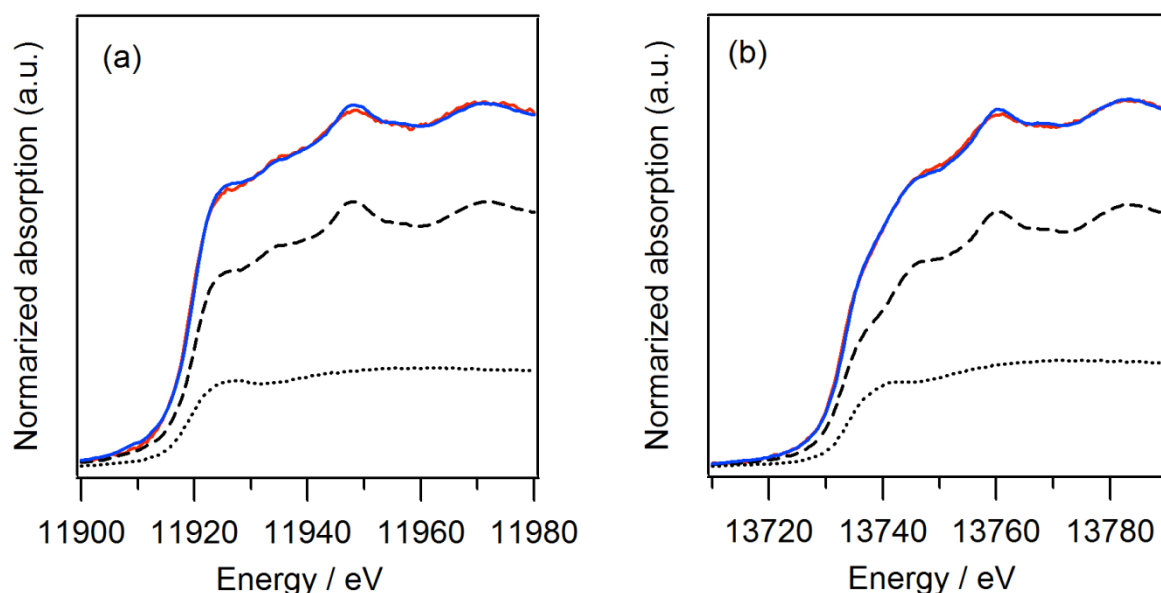

Figure 4. Measurement XANES spectra at ca. 180 s (red solid line) with the synthesized spectra (blue solid line) using the linear combination of those of the Au nuclei at 3.6 s (dotted line) and the Au foil (dashed line) at (a) the Au L_3 and (b) L_2 edges.
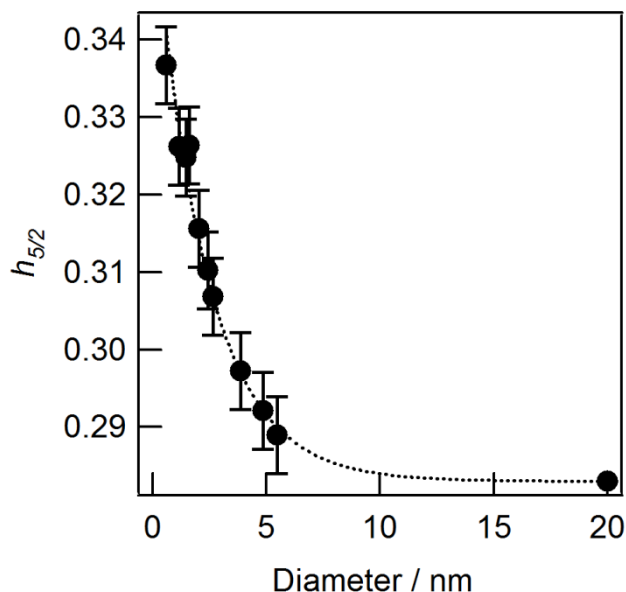
Figure 5. Variation in the value of $h_{5/2}$ with the diameter calculated from dispersion evaluated from XANES spectral analysis.

Conclusion

Formation of AuNPs in the presence of DT was observed *in situ* by QXAFS spectroscopy at the Au L_3- and L_2-edges. The spectra of small AuNPs during particle growth represented higher absorption intensity around the edges in comparison with that of Au foil. XANES spectral analysis revealed that the higher absorption intensity was mainly due to Au–S scatterings and slightly due to *d* band vacancies of Au metal species. The slight contribution of *d* band vacancies was not observed in the value of $h_{3/2}$ because of the much larger contribution of Au–S scatterings than of the vacancies in the $d_{3/2}$ state. On the other hand, the value of $h_{5/2}$ reflected the contribution of *d* band vacancies under the large contribution of Au–S scatterings. The variation in the value of $h_{5/2}$ with the size of AuNPs indicated that the intrinsic properties of the AuNPs deviated from the size.

References

[1]   R.C. Jin, Nanoscale 2 (2010) 343.

[2]   M. Haruta, Catal. Today 36 (1997) 153.

[3]   M. Hu, J. Chen, Z.-Y. Li, L. Au, G.V. Hartland, X. Li, M. Marquez, and Y. Xia, Chem. Soc. Rev. 35 (2006) 1084.

[4]   H. Tsunoyama, N. Ichikuni, H. Sakurai, and T. Tsukuda, J. Am. Chem. Soc. 131 (2009) 7086.

[5]   M. Brust, M. Walker, D. Bethell, D.J. Schiffrin, and R. Whyman, Chem. Commun. (1994) 801.

[6]   J. Ohyama, Y. Hitomi, Y. Higuchi, M. Shinagawa, H. Mukai, M. Kodera, K. Teramura, T.

Shishido, and T. Tanaka, Chem. Commun. (2008) 6300.

[7]   B.V. Enüstün, and J. Turkevich, J. Am. Chem. Soc. 85 (1963) 3317.

[8]   G. Schmid, B. Boese, R. Pfeil, F. Bandermann, S. Meyer, G.H.M. Calis, and J.W.A. van der Velden, Chem. Ber. 114 (1981) 3634.

[9]   T. Yonezawa, K. Yasui, and N. Kimizuka, Langmuir 17 (2001) 271.

[10]   Y. Hitomi, J. Ohyama, Y. Higuchi, K. Aoki, T. Shishido, T. Funabiki, M. Kodera, and T. Tanaka, Bull. Chem. Soc. Jpn. 83 (2010) 1392.

[11]   A.N. Mansour, J.W. Cook, and D.E. Sayers, J. Phys. Chem. 88 (1984) 2330.

[12]   K. Ebitani, T. Tanaka, and H. Hattori, Appl. Catal. A 102 (1993) 79.

[13]   D. Zanchet, H. Tolentino, M.C.M. Alves, O.L. Alves, and D. Ugarte, Chem. Phys. Lett. 323 (2000) 167.

[14]   P. Zhang, and T.K. Sham, Appl. Phys. Lett. 81 (2002) 736.

[15]   P. Zhang, and T.K. Sham, Phys. Rev. Lett. 90 (2003) 245502.

[16]   M.A. MacDonald, P. Zhang, H. Qian, and R. Jin, J. Phys. Chem. Lett. 1 (2010) 1821.

[17]   J. Ohyama, K. Teramura, Y. Higuchi, T. Shishido, Y. Hitomi, K. Kato, H. Tanida, T. Uruga, and T. Tanaka, ChemPhysChem 12 (2011) 127.

[18]   D.G. Duff, A. Baiker, and P.P. Edwards, Langmuir 9 (1993) 2301.

[19]   T. Uruga, H. Tanida, K. Inoue, H. Yamazaki, and T. Irie, AIP Conf. Proc. 882 (2007) 914.

[20]   G.H. Woehrle, M.G. Warner, and J.E. Hutchison, J. Phys. Chem. B 106 (2002) 9979.

[21]   R.E. Benfield, D. Grandjean, M. Kroll, R. Pugin, T. Sawitowski, and G. Schmid, J. Phys. Chem. B 105 (2001) 1961.

[22]   P.J.G. Goulet, and R.B. Lennox, J. Am. Chem. Soc. 132 (2010) 9582.

[23]   C.C. Tyson, A. Bzowski, P. Kristof, M. Kuhn, R. Sammynaiken, and T.K. Sham, Phys. Rev. B 45 (1992) 8924.

[24]   H. Hakinen, R.N. Barnett, and U. Landman, Phys. Rev. Lett. 82 (1999) 3264.

[25]   L.F. Mattheiss, and R.E. Dietz, Phys. Rev. B 22 (1980) 1663.

[26]   E. Bus, J.T. Miller, and J.A. van Bokhoven, J. Phys. Chem. B 109 (2005) 14581.

[27]   T. Kubota, K. Asakura, N. Ichikuni, and Y. Iwasawa, Chem. Phys. Lett. 256 (1996) 445.

[28]   T. Kubota, K. Asakura, and Y. Iwasawa, Catal. Lett. 46 (1997) 141.

[29]   M.K. Oudenhuijzen, J.A. van Bokhoven, J.T. Miller, D.E. Ramaker, and D.C. Koningsberger, J. Am. Chem. Soc. 127 (2005) 1530.

[30]   M.G. Samant, and M. Boudart, The Journal of Physical Chemistry 95 (1991) 4070.

[31]   A.V. Soldatov, S. Della Longa, and A. Bianconi, Solid State Commun. 85 (1993) 863.

[32]   K. Nobusada, J. Phys. Chem. B 108 (2004) 11904.

[33]   M. Comotti, C. Della Pina, R. Matarrese, and M. Rossi, Angew. Chem. Int. Ed. 43 (2004) 5812.

[34]   M. Okumura, Y. Kitagawa, M. Haruta, and K. Yamaguchi, Chem. Phys. Lett. 346 (2001) 163.

[35]   F. Boccuzzi, A. Chiorino, M. Manzoli, P. Lu, T. Akita, S. Ichikawa, and M. Haruta, J. Catal. 202 (2001) 256.

[36]   M. Haruta, The Chemical Record 3 (2003) 75.

[37]   T. Hayashi, K. Tanaka, and M. Haruta, J. Catal. 178 (1998) 566.

[38]   M. Valden, X. Lai, and D.W. Goodman, Science 281 (1998) 1647.

[39]   D.A.H. Cunningham, W. Vogel, H. Kageyama, S. Tsubota, and M. Haruta, J. Catal. 177 (1998) 1.